



## Preparation and Evaluation of Mechanical and Physical Properties of Random Silica Fiber/Modified Resole Resin Composites

Issam Elwan<sup>1\*</sup> and Rafi Jabra<sup>2</sup>

<sup>1,2</sup> Department of Applied Physics, Higher Institute for Applied Sciences and Technology (HIAST), P.O. Box 31983, Barzah, Damascus, Syria.

Received 9 Jan 2017,  
Revised 8 Feb 2017,  
Accepted 11 Feb 2017

### Keywords

- ✓ Composite material,
- ✓ mechanical properties,
- ✓ phenolic resin,
- ✓ resole resin,
- ✓ short silica fiber reinforced polymer,

[issam42003@gmail.com](mailto:issam42003@gmail.com)  
(Issam Elwan);  
+963966602799

### Abstract

In this study, composites of short silica fibre (SSF) and modified ammonium phenolic resole resin (MRR) were prepared by blending of ammonium phenolic resole resin with 15phr polyvinylbutyral (PVB). Different weight ratio of short silica fiber (SSF) reinforced (PVB) modified resole phenolic resin composites were fabricated. FTIR was used to study the chemical structure of modified and unmodified resole resin. Thermal decomposition of MRR and SSF/MRR composites were investigated with differential scanning calorimetry (DSC) and thermogravimetric analysis (TGA). Tensile, flexural and impact strength tests of the composites were conducted to investigate the effect of SSF content on SSF/MRR composites. The interaction between fiber and resin was studied by scanning electron microscope (SEM) and optical microscopy. The results showed that SSF/MRR composites were prepared through simple and low-cost hot-compression molding without using interfacial promoting bonding agent and that MRR matrix can be loaded up to 65wt% short silica fibres. A good PVB and resole resin (mixture of 85 % resole resin and 15 % PVB) compatibility was confirmed by FTIR and DSC. The mechanical properties such as tensile strength (28.4MPa), flexural strength (155.03MPa), flexural Young's modulus (12.81GPa), and impact strength (42.04KJ/m<sup>2</sup>) of SSF/MRR composites showed optimum value at 55wt% fibre content. Deformation and fracture behavior of SSF/MRR composites were also investigated and correlated with the mechanical property data and microscopic examination. Water absorption, void content and density of composites were also determined.

### 1. Introduction

The best mechanical properties of fibre reinforced polymer composites are obtained from continuous fibre reinforcement but such materials cannot be fitted easily to mass production. So it could be substituted by another forms like short fibre reinforced composites which can be processed in a manner similar to the matrix and permitting mass production of components with quite complicated shapes in a number of different ways to a certain extent. The properties of short fibre-polymer composites are strongly dependent on the fibre volume fraction and on the fibre orientation distribution also on adhesion between the fibre and the matrix [1]. Although Short-fiber reinforced polymer (SFRP) composites are widely used for industrial applications due to their versatile properties such as low cost, lightweight, ease of fabrication, and good mechanical properties [2-3]. Phenolic composites provide some excellent characteristics like flame retardation, low smoke generation, and relatively high-temperature resistance.

Silica-phenolic composite systems are also suitable candidates as ablative materials [4-7]. In general, a high fiber content is required in order to achieve a high-performance SFRP composite. Therefore, the effect of fiber content on the mechanical properties of SFRP composites is of particular interest and significance [8-10]. Phenolic resin type ammonium resole resin is the product of alkali condensation reaction of phenol and formaldehyde with water as by-product [11]. High cross-linked structure formed by the molding process of phenolic resins under heat and pressure. This structure yields excellent dimensional and thermal stability with superior load-bearing capability at elevated temperatures [12]. However, high degrees of cross-linking generally lead to non-desirable brittleness which could be mitigated by resin modification to impart flexibility [13-15]. Verma, A .P. et al.[16] found that the modification of phenolic resin by polyvinylbutyral (PVB) not only improved ductility of the resin and impact resistance, but also the wear resistance of the composite and its tensile modulus. In this context, phenolic resin modified PVB showed a significant increase in impact resistance [17-18]. As phenolic resins are compatible with a variety of reinforcements, a wide range of phenolic engineering composite materials can be synthesized with varying properties. Among various reinforcing fibres, silica fibres have attracted more and more interest because of their

excellent dielectric properties, high-temperature stability, thermal shock resistance, chemical stability and ablation resistance. In recent decades, these fibres have been used to fabricate high-temperature electromagnetic window materials to meet the requirements of communication and control and thermal protection in aerospace applications [19-20]. Silica fibres are available in the form of mats, tapes, clothes, continuous and short filaments, roving, and yarns [21-22]. It has been shown by Sabu Thomas et al. [23], that glass fibre effectively reinforces in PF resin and mechanical performance is maximum at 40 wt% fibre loading. Hin et al. [24] have presented a numerical simulation of the effects of fibre length distribution on the elastic and thermo-elastic properties of short fibre composites. Fu et al. [25] have studied the flexural properties of misaligned short fibre reinforced polymers taking into account the effects of fibre length and fibre orientation. G. Venkata Reddy et al. [26] reported that a fiber length of 20 mm and fiber loadings of 40 wt% were found to be optimum for the best mechanical properties of coir/glass fiber phenolic resin based composites. Botev et al. [27] investigated the mechanical properties of short basalt fibre-reinforced polypropylene with different fibre contents. They found that mechanical characteristics, stress and strain at yield, increase with increasing fibre content, impact strength also rises up to fourfold higher than that of unfilled polypropylene. In general, short-fibre/polymer matrix composites are much less resistant to fatigue damage than the corresponding continuous-fibre-reinforced materials [1,28].

The present work deals with the preparation of composite materials based on SSF reinforced modified resole phenolic resin. Four composites with 20/80, 40/60, 55/45, and 65/35 fiber to resin weight ratios were prepared using compression molding technique. The effect of SSF content on mechanical and physical properties of the phenolic matrix was examined.

## 2- Experimental details.

### 2-1- Materials.

PVB was purchased from Wacker Company with butyral and hydroxyl content of 80 wt% and 18±1.5 wt% respectively [29]. Silica cloth woven fabric manufactured by Shandong Chuangjia New Materials Co. Ltd. was used as reinforcement raw material and the properties are shown in table 1. Industrial grade phenol (98%), Analytical grade sulphuric acid (98%), formalin (37% formaldehyde), ammonium hydroxide (25%) and ethanol were purchased from Sigma–Aldrich.

**Table 1.** Properties of silica cloth woven fabric [30].

Weave	Satin 8/3
Surface density(g/m <sup>2</sup> )	610
Thickness (mm)	0.6
Filament diameter, μm	9
Width (cm)	92
SiO <sub>2</sub> content	96 %min.
Elongation at break (%)	0.5

### 2-2- Experimental procedure.

Phenolic resole resin was synthesized with ammonia as catalyst and formaldehyde / phenol 1.25molar ratio [11]. A four necks round bottom flask equipped with mechanical stirrer, temperature controller and condenser was charged with 1 mole of phenol, 1.25 mole of 37% aqueous formaldehyde solution and 4.7 g of 25% ammonia solution. The solution was stirred and refluxed for 75 min at 85°C. Then pH value was adjusted to 6-7 by the addition of 5% sulfuric acid solution. The aqueous phase was decanted, and the rest of water was removed by distillation under reduced pressure for about 2h at 60°C. The physical properties of prepared ammonia resole resin are tabulated in Table 2.

**Table 2.** Physical properties of synthesized phenolic resin.

Property	Value
Solid content, %	75-79
Physical form	Clear brown liquid
Content of free phenol, %	6.41
Content of free formaldehyde, %	3.25
Gel time at 150°C	110 sec
Density (g/cm <sup>3</sup> )	1.12
pH	7.2-7.8

### 2-3- Matrix preparation.

The prepared phenolic resin type resole was blended with PVB 15 parts per hundred (phr) weight of PVB resin using ethanol as a solvent. Blending was done in the chemical reactor at 30 °C and stirrer speed of 250 rpm for 2 hours. The viscosity is measured using Forde cup Ø4mm (DIN-4) and can be adjusted to 45-50 s by adding absolute ethanol.

### 2-4- Fabrication of fibre reinforced composites.

Silica fibers were separated from silica cloth weave fabric and cut with a lengths of 5-30 mm. The SSF were mixed with the modified resole resin in different fiber to resin ratios, 20/80, 40/80, 55/35, and 65/35 % by weight. After thorough mixing, the resin-impregnated fibers were partially cured at 65 ± 5 °C for 8h in an oven. After that, the SSF/MRR mixtures were dried at 70 °C in a vacuum oven for 6h. The final product is depicted in Figure 1. This product was later used for making hot- compression molded test specimens for mechanical and physical testing. Compression molding used electrically heated hydraulic press of 100 tons capacity. The SSF/MRR composites were fabricated by hot compression molding under curing pressure of 10 MPa and a temperature of about 175±5°C for 8-12 minutes depending on sample thickness.



**Figure 1.** SSF/MRR composite blend before pressing.

### 2-5- Physical properties tests.

Water absorption test, density and porosity of the prepared composite were determined as follows:

#### 2-5-1- Water absorption test.

Water absorption studies were performed according to the ASTM D570-98 method. Sample weight was first determined as  $m_0$ , then samples were submerged in distilled water at room temperature and periodically taken out and weighted immediately after wiping out the surface water using Sartorius™ balance until constant weight  $m$ . The percentage of absorbed water can be calculated according to the following equation (Eq. 1) [31]:

$$\text{Total Moisture Content} = \frac{m - m_0}{m_0} \times 100 \quad 1$$

#### 2-5-2- Density measurement.

The density of the SSF/MRR composites samples were determined at room temperature by Archimedes method using distilled water (density = 1.0 kg.m<sup>-3</sup> at 20°C) as a wetting fluid and the above-mentioned balance. By this method, dried cubic sample mass was determined as  $m$ , then the immersed sample mass in distilled water was measured as  $m_1$ . The density  $\rho$  can be calculated according to following equation (Eq. 2):

$$\text{Density } (\rho) = (m / (m - m_1)) * \rho_w \quad 2$$

Where,  $\rho_w$  is distilled water density at the ambient measurement temperature.

#### 2-5-3- Determination of composite theoretical density.

Theoretical composite density ( $\rho_{th}$ ) can be calculated according to following equation ( Eq. 3) [32].

$$\rho_{th} = 100 / \left( \frac{W_p}{\rho_p} + \frac{W_r}{\rho_r} \right) \quad 3$$

Where:  $W_p$ : resin weight fraction in the composite;  $\rho_p$  : resin density;  $W_r$ : reinforcement weight fraction in the composite;  $\rho_r$  : reinforcement density.

2-5-4- Determination of composite porosity.

The porosity  $V_p$  of the composite can be calculated according to following equation (Eq. 4) [32]:

$$V_p = \left\{ \frac{\rho_{th} - \rho_{exp}}{\rho_{th}} \right\} * 100 \quad 4$$

Where  $V_p$  : porosity %;  $\rho_{th}$  and  $\rho_{exp}$ : composite theoretical and measured density.

### 3- Mechanical property tests.

3-1- Tensile test.

The test was conducted according to ASTM D3039-74 standard with sample narrow section dimensions of 75x10x4mm. The test was carried out at room temperature on 5 samples for each composite using a universal testing machine [ADAMEL LHOMARGY, France] having a capacity of 10 KN at a cross head speed of 5mm/min. The test piece was properly mounted and monolithically loaded until fracture.

3-2- Flexural test.

Three point flexural test was performed in accordance with ASTM D790-03 test method to measure flexural properties of the composite samples. The test were carried out at room temperature on 5 samples for each composite using the same universal testing machine. Flexural samples measured 120x10x4mm, span length was 100mm and deformation speed was 5mm/min. Samples were tested at room temperature in replicates of five each.

3-3- Impact test.

The impact resistance of the composite was carried out using Charpy impact testing machine according to ASTM D 256-73 standard. Impact test samples in number of 5 were prepared using hot press molding technique and tested at room temperature by a single swing pendulum hammer impact tester (Model JBW-300). The specimen size was 55x15x11mm with depth under notch of 9.8mm.

### 4- Thermal Properties.

4-1- TGA and DSC test.

Thermal stability of SSF/MRR composites and matrix carbonization with respect to temperature were evaluated using a thermogravimetric analyzer (TGA) and differential scanning calorimetric (DSC) (SETARAMLABSYS evo TGA 1150 Instruments, France) as per ASTM E1868. The heat generation rates in the dynamic scanning with respect to the temperature was measured by DSC test. Samples from 10-20 mg were secured from 30°C to 1200°C at a heating rate of 10°C/min. The TGA and DSC tests were performed in normal atmosphere environments and in nitrogen ( $N_2$ ) separately. According to the initial sample weight and degradation temperature, sample % char was noted.

### 5- FTIR spectroscopic analysis.

FTIR spectra of ammonium phenolic resole resin, PVB and MRR matrix powder samples were analyzed using a Bruker Vector 22 FTIR Spectrometer with a standard DTGS detector and KBr window. The infrared experimental conditions were 6 scans and 1  $cm^{-1}$  resolution. The samples were prepared according to KBr pellets/disks method for solid samples.

### 6- Morphology characterization.

6-1- Optical microscopy examination.

Transmission and reflection metallurgical microscope equipped with a camera (Model XJZ-6 upright, China) was used to examine the morphology of the SSF/MRR composites. The samples were sectioned and mechanically ground on emery paper grade of (60–800 grits) using water as coolant. The ground specimens were polished using a suspension of one-micron size alumina polishing powder in distilled water. Final polishing was done using 0.5 micron alumina polishing powder.

6-2- Scanning electron microscopy (SEM) examination.

The nature of the adhesion between matrix and fiber and correlation relating structure to mechanical properties can be obtained by SEM assessment of the composite fracture surface. The fracture surface morphology of SSF/MRR composite samples was examined using a scanning electron microscope (SEM) (VEGA II XMU from TESCAN company, USA). Prior to analysis, all the samples fracture surfaces were coated with Palladium using a sputtering system to eliminate electric charging during SEM analysis.

## 7- Results and Discussion.

### 7-1- Infrared analysis.

Figure 2 (A, B, and C) shows of FTIR results of ammonium resole phenolic resin cured at 160°C for 1 h (Figure 2A) FTIR spectrum of PVB (Figure 2B) and FTIR spectrum of MRR (Figure 2C).

The attribution of the main characteristic absorption peaks has been done based on [33-34]. The FTIR spectrum of the resole resin (Figure 2A) shows a broad high intensity band at around 3300  $\text{cm}^{-1}$  associated with the -OH groups (phenolic OH and methylol groups OH), the peak found at 2977  $\text{cm}^{-1}$  could be attributed to methylene groups. The peak associated with stretching vibrations of C=C bond of the aromatic ring are found at around 1600  $\text{cm}^{-1}$ . The peak at 1477  $\text{cm}^{-1}$  was attributed to flexural vibration of CH<sub>2</sub> groups. Figure 2 also shows absorption bands at around 1240  $\text{cm}^{-1}$  and 1045  $\text{cm}^{-1}$  which are related to stretching of C-O groups in phenol and methylol respectively. The peaks at 881  $\text{cm}^{-1}$ , 755  $\text{cm}^{-1}$  and 694  $\text{cm}^{-1}$  corresponds to mono, ortho and para substituted phenyl rings respectively.

The structure of PVB polymers were investigated by many authors and functional groups corresponding to the major peaks of PVB infrared spectra have been identified [35]. As can be seen from Figure 2B, a broad and strong band appeared with a maximum at around 3365  $\text{cm}^{-1}$ , this peak is attributed primarily to both symmetric and asymmetric OH stretching vibrations. The band at around 2974  $\text{cm}^{-1}$  can be assigned to aliphatic C-H stretching, while the peak at 1675  $\text{cm}^{-1}$  can be assigned to C=O carbonyl stretching. The band appeared between 1396 and 1460  $\text{cm}^{-1}$ , with a maximum at around 1383  $\text{cm}^{-1}$  belongs to flexural stretching of CH<sub>2</sub> and CH<sub>3</sub>. The bands appearing between 1090 and 1050  $\text{cm}^{-1}$  can be attributed to C-O-C stretching. The sharp peak at 881  $\text{cm}^{-1}$  can be ascribed to C-C and C-O stretching and also to flexural stretching of C-C-H and O-C-H.

The infra-red spectra of PVB modified ammonium resole resin (MRR) thermally treated at 160°C for 1 h is represented in Figure 2C. The FTIR spectrum shows the presence of a wide broad band 3425  $\text{cm}^{-1}$  corresponding to the -OH group. This peak was assigned either to the non-associated free hydroxyl groups or to the formation of hydrogen bonds between the OH groups of PVB and resole resin [33]. The weak band at 2980  $\text{cm}^{-1}$  (C-H stretching) is declining with comparison with both resole resin FTIR spectra and that of PVB. This is due to the decrease of etherification reactions between the methylol groups as explained by C. Nirmal et al. [36]. The bands corresponding to the ether groups (1100-1200  $\text{cm}^{-1}$ ) becoming less intensive in the modified resole resin spectra indicate that ether groups have interacted with the phenolic -OH groups [33-34].

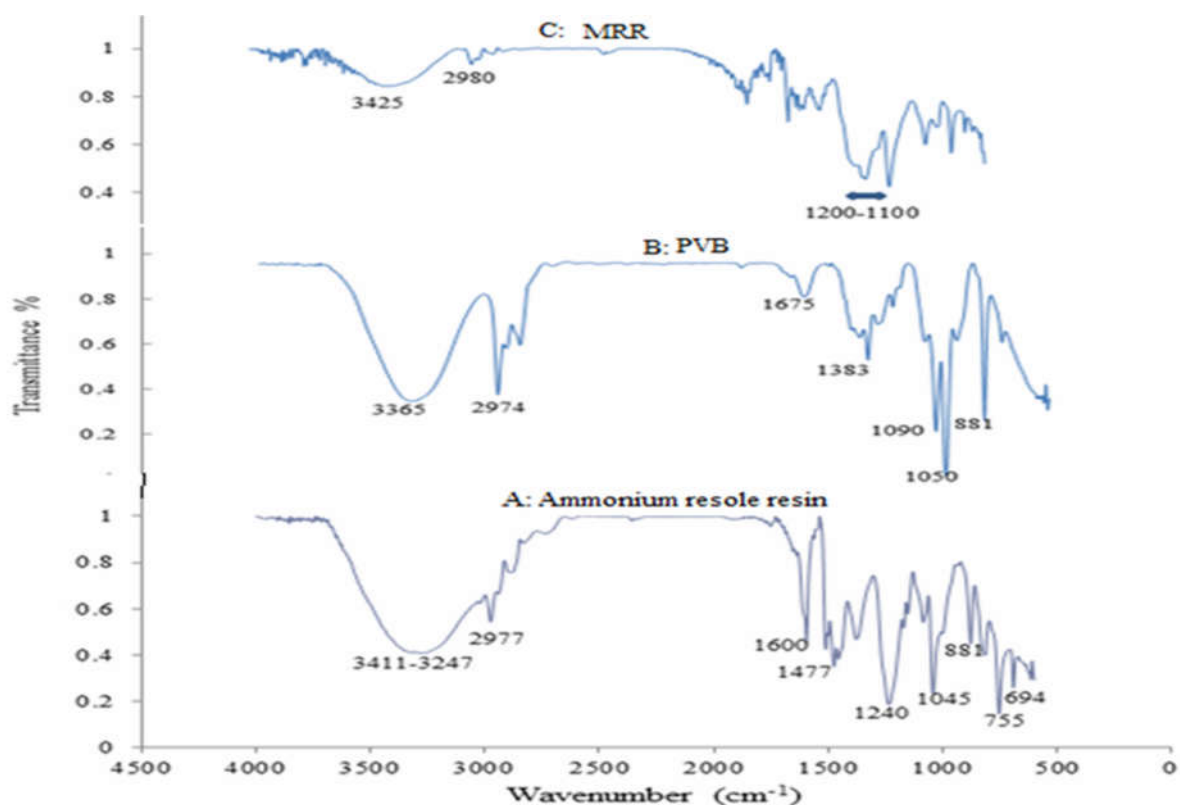


Figure 2. FTIR spectrum of (A) cured resole resin, (B) PVB, and (C) MRR.

7-2- Mechanical properties results.

**Table 3.** Results of tensile, flexural, and impact testing for each of SSF/MRR composite as a function of silica fibre content.

Silica fibre content (wt%)	Tensile strength (MPa)	Tensile modulus of elasticity (MPa)	Flexural strength (MPa)	Flexural modulus of elasticity (GPa)	Impact resistance (KJ/m <sup>2</sup> )
20	15.64	1047.5	28.44	4.59	2.61
40	26.05	1066.8	42.41	6.99	9.18
55	28.4	1542.3	155.03	12.81	42.04
65	27.6	1509.8	27.57	5.14	12.25

7-2-1- Tensile strength.

The stress-strain curves of SSF/MRR composites exhibit a brittle fracture and show no significant deviation from linearity shown in Figure 3. This behaviour is related to the linear brittle behaviour of both resole matrix and silica fibers.

It is observed that the tensile strength increases with increasing fiber content up to 55% (28.4 MPa) weight ratio and slightly decrease at 65 wt% to 27.6 MPa as shown in Figure 4. This slight reduction in tensile strength of the SSF/MRR composites can be attributed to relative decreasing of matrix amount promoting adhesion force against shear fracture of fiber/matrix interface under load, to improper wetting process [37] and to fibres entanglement and clustering as evidenced by microscopic examination (Figure16-i).P. Amuthakkannan et al. [6] study demonstrated that fibre weight ratio and length were of substantial effect on the increase in tensile strength of the polyester/basalt fibre composites. Their investigations showed that the optimum fibre weight percentage and optimum fibre length were 68 wt% and 10 mm respectively.

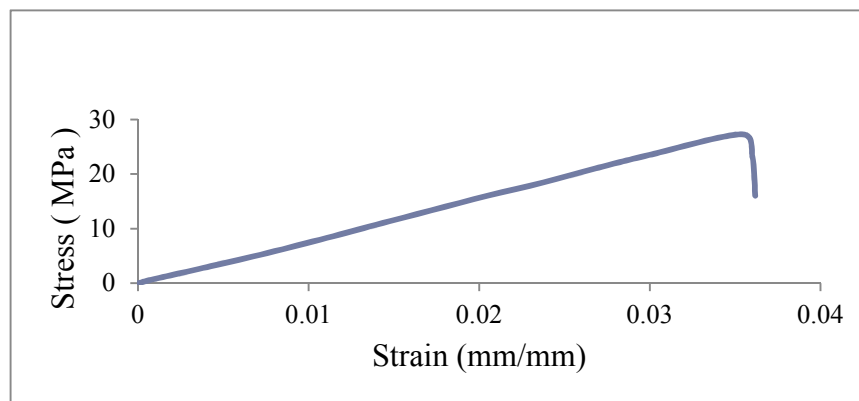


**Figure 3.** Stress-strain curve of SSF/MRR composites.

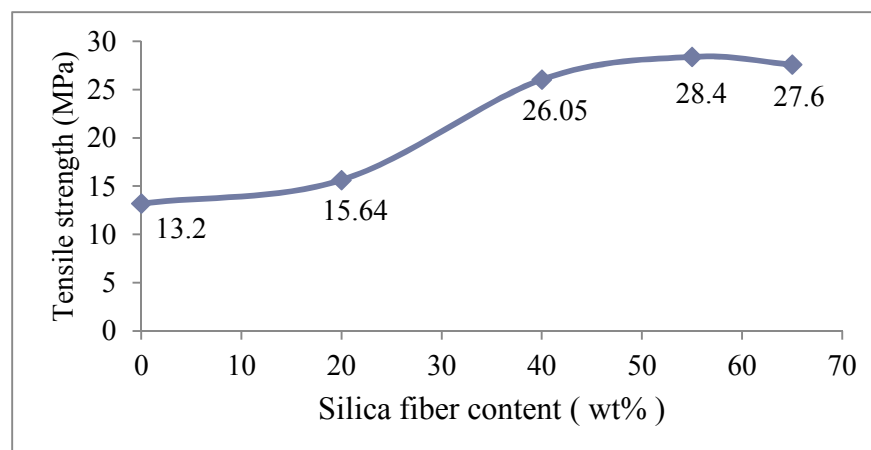


**Figure 4.** Tensile strength of SSF/MRR composite versus short silica fibre content.

### 7-2-2- Tensile Young's modulus.

From Figure5. it can be seen that the Young's modulus of SSF/MRR composites is increasing with fibre weight percentage up to 55wt% (1542.3 MPa) and then slightly dropping at 65 wt% (1509.8 MPa). It appears that the addition of 55 wt% SSF to modified resole resin increases Young's modulus by 69% in comparison with 20 wt% and 40 wt% of SSF content in line with tensile strength results.

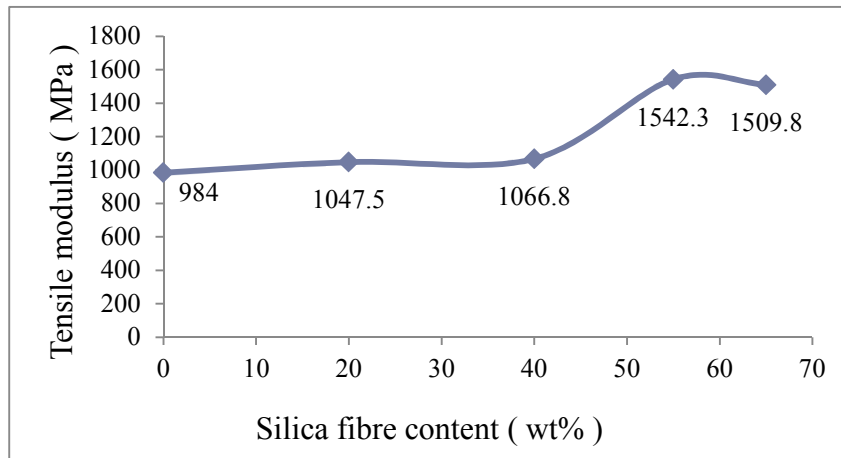


**Figure 5.** Tensile Young's modulus of SSF/MRR composites with silica fiber content

### 7.2.3. Tensile strain.

As seen in Figure6, the strain at break of SSF/MRR composites increases with increasing silica fiber content. Strain at break of 1.37% for modified resole resin increased to 4.19% at silica fiber ratio of 55 wt%, then slightly dropped to 3.61% at 65 wt%. This result is in harmony with what S.Thomas [23] obtained in phenolic resin/short glass fiber composites. It can be concluded that short silica fiber improved slightly the strain at break without changing the brittle behaviour [38] because both silica fibers and modified resole resin are of brittle behaviour. Short silica fibers reinforced the modified resole resin and delayed slightly the composite fracture. The quality of the modified resole resin-silica fibers interface is expected to play detrimental role in the composite failure, poor bonding between silica fibre and matrix leads to poor mechanical properties. SEM images (Figure16: d- e-f) indicates cases of clean fiber surface induced by fibre pull-out events.

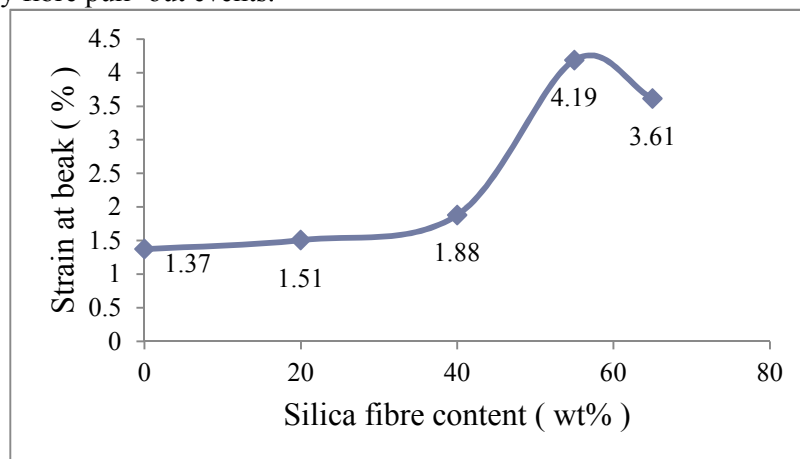


**Figure 6.** Strain at break variation of SSF/MRR composites with silica fiber content.

### 7-3- Flexural test results.

It could be observed (Figure 7) that all SSF/MRR composites exhibit before failure, a similar linear and elastic behavior, but as fibre loading increases the plastic deformation region at higher strain becomes apparent 20 wt% and 40 wt% of SSF/MRR composites show sudden drop in stress at fracture while 55 and 65 wt% of SSF/MRR composites show gradual drop in stress before fracture. The range of strain increases with resole content decrease. After failure, the brittle character of these composites is dominated by the matrix fraction, the higher this fraction, the steeper is the composite de-loading.

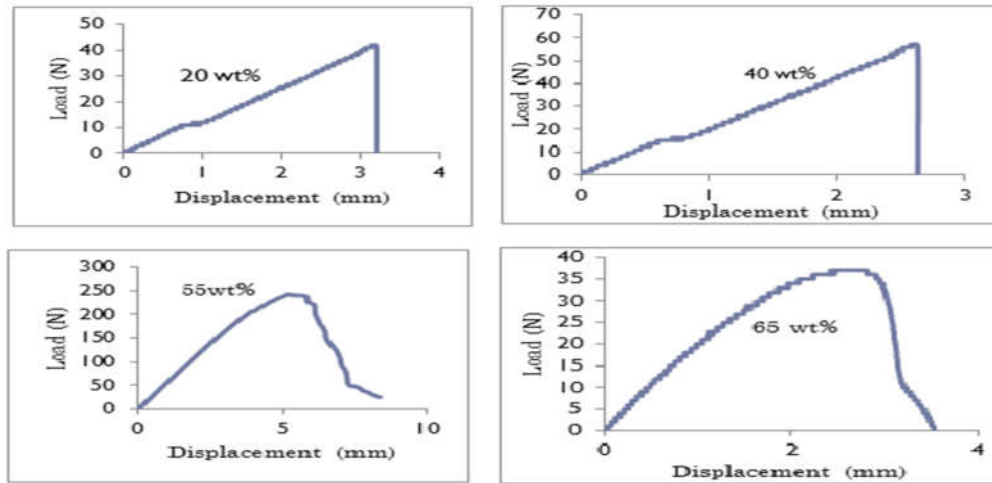


**Figure 7.** Flexural force- deflection behavior of SSF/MRR composites at different fibre loading (wt%).

### 7-3-1- Flexural strength.

Flexural strength of SSF/MRR composites exhibits clearly a maximum value (155.03 MPa) at 55 wt% silica fibre and decreases beyond that fibre fraction as shown in Figure 8. Compared with investigation of K. S. S. Kumar et al.[37] showed that an increase in the proportion of short carbon fibre loading (fibre length 20mm) improved the flexural and tensile properties of composite until 50-60 wt% of fibre.

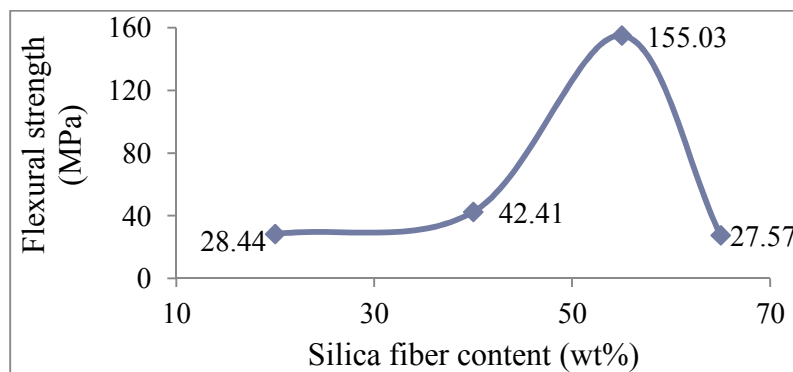


**Figure 8.** Flexural strength of SSF/MRR composites with silica fibre content.

Generally, it is known that the failure of the composites can be attributed to weak bonding between fiber and matrix, presence of voids that leads to fiber and matrix fracture and fiber pull-out.

### 7-3-2- Flexural Young's modulus.

As shown in Figure 9, as the content of silica fibre is raised, the E modulus of the composite increases and reaches a maximum value of 12.81 GPa at 55 wt%, then E falls to 5.14 GPa at 65 wt%.

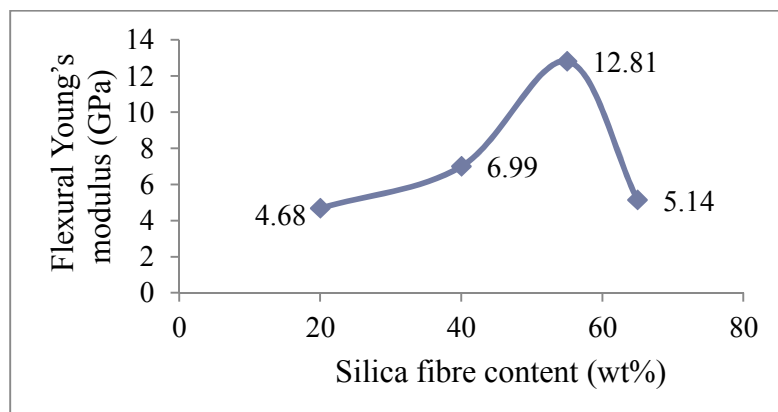


**Figure 9.** Flexure Young's modulus of SSF/MRR composites with silica fibre content.

#### 7-4- Impact resistance.

The impact resistance of neat resin was 2.59 KJ/m<sup>2</sup>, near that of 20 wt% fiber composite. When the composite contains 55 wt% silica fibre, the impact resistance reaches the maximum value of 42.04 KJ/m<sup>2</sup> and decreases to 12.25 KJ/m<sup>2</sup> at 65 wt% silica fibre. Figure10 illustrates that the impact resistance increased with increasing filler loading up to 55 wt% then slumps. The higher the fiber content, the more difficult to disperse them uniformly in the matrix. Figure16 (a, b) shows that the SEM images of fractured surface of composites with 65 wt% SSF. It can be seen that silica fiber aggregated inside the composite and smashed under hot pressing. The aggregations of fiber at high content weaken the bond strength of fiber/matrix interface, and then weaken the energy consumption ability of silica fibers which consume fracture energy by fiber de-bond and pull-out, ultimately resulting in the decrease of impact strength. The impact resistance of composites is governed mainly by two factors [39]: first, the capability of the fibre to absorb energy that can delay crack propagation and second, poor interfacial bonding which induces micro-spaces between the fibres and the matrix, resulting in less resistance to crack propagation.

S. Thomas et al.[38] have compared the mechanical properties of phenol formaldehyde composites reinforced with banana fibres and glass. They found that the impact resistance of the composite is increasing with fibre weight fraction in both banana fibre composites and glass fibre composites. They also showed that the impact strength of 40%wt glass fibre reinforced resole is found to be 700% higher than pure resole. V. Sebrekoska et al.[40] studied short carbon fibres and an ablative phenol–formaldehyde resin for high temperature application. They observed that impact strength is higher for the composites with the longer fibers length (50 mm) comparing with 25 mm fiber length and with 57wt% fiber loading.

Conclusively, an optimum fiber content seems to appear from impact absorption energy and is determined by the relative contribution of each impact energy dissipation mechanism, fibre–matrix debonding, fibre fracture, fibre pull-out and matrix plastic deformation.

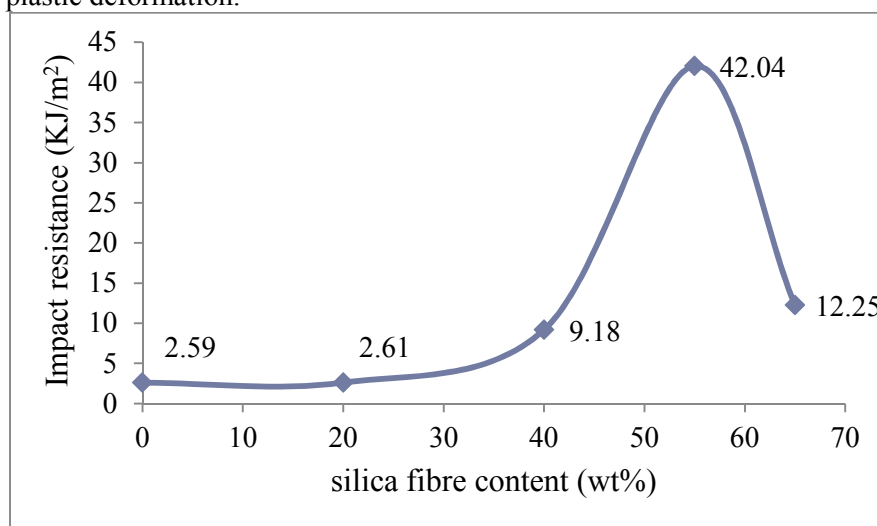


**Figure 10.** Impact resistance of SSF/MRR composites with silica fibre content.

#### 7-5- Thermogravimetric Analysis.

The chemical changes of SSF/MRR composite exhibits a three-stage decomposition as shown in Figure11. First zone (50°C ~ 300°C) is assigned to the loss of weakly-bonded water from modified phenolic resole resin and post cure volatilization of unreacted phenols, carbon dioxide and monomers in the resin. The weight loss was insignificant (about 1.4%). The second zone (300°C ~ 650°C) is related to the beginning of thermal degradation and decomposition of cured modified phenolic resole resin by scission reaction of the polymer and the weight loss is (~15.7%). Finally, carbonization zone and char formation (over 600°C) occurs with formation of H<sub>2</sub>, CO, and CH<sub>4</sub>. In this step the aromatic rings of the phenolic resole resin turn into carbonized char by dehydrogenation and hydrogen transfer reaction, the corresponding weight loss could be attributed to bulk degradation of phenolic resole resin matrix [41-42]. Above 1000°C, no significant increase in mass loss is observed because all phenolic resin in the composite has been carbonized and SSF/MRR composite residue reach 74% approximately at 1150°C.

The simplified illustration of the carbonized structure might be represented by Figure 12. As long as SSF fiber does not decompose at higher temperatures, so only modified phenolic resole resin is fully carbonized and transformed into char via dehydrogenation and condensation reactions. This char layer improves thermal protection of silica fibre. Thus, SSF/MRR composite is considered as good thermal protection material.

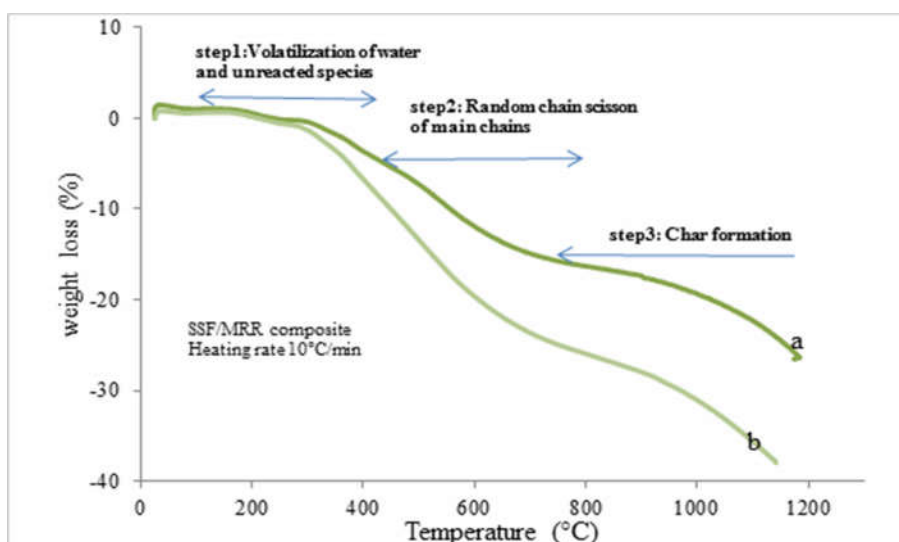


**Figure 11.** TGA curves for SSF/MRR composites, showing different regions of decomposition and condensation under nitrogen (a) and air flow (b).

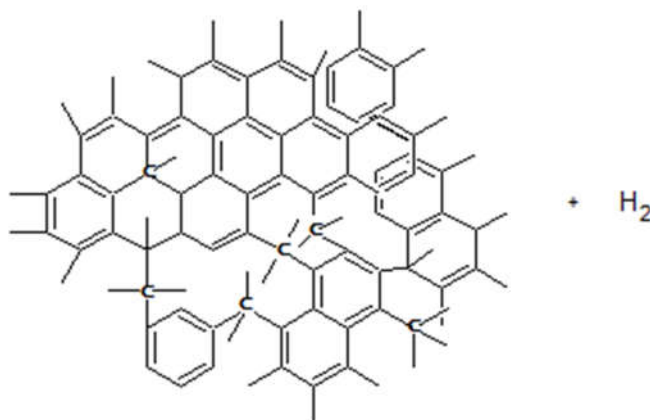


**Figure 12.** Schematic representation of suggested structure for fully carbonized phenolic resin within highly cross-linked glassy network.

#### 7-6- DSC analysis.

In order to identify the curing process and heat generation rates of SSF/MRR composites and modified resole resin systems, they were subjected to DSC analysis (with 10°C/min) in a nitrogen (N<sub>2</sub>) environment and their corresponding thermograms are shown in Figure 13(a, b).

From Figure 13(a, b), the endothermic peak around 100°C in the DSC curve of modified resole resin can be regarded as the evaporation of the residual solvent, ethanol, and reaction generated water which is the byproduct of the condensation reaction of phenol and aldehyde. The fact that this peak is very weak in DSC thermogram of SSF/MRR composites could be attributed to the heat treatment during hot pressing molding of the composites before DSC test. Figure 13 shows that the curing of modified resole resin and SSF/MRR composites are both initiated at around 150°C. This value was chosen as the point where the exothermic curve deviates from the baseline towards higher values. Modified resole resin thermogram exhibit three exothermic peaks at around 274°C, 380°C, and 496°C. These peaks correspond to the heat of curing ( $\Delta H_{\text{curing at } 274^{\circ}\text{C}}$ ) of -22.81 J/g and -535.49 J/g for the first two peaks. The third one is related to the degradation of modified resole resin matrix. On the other hand, SSF/MRR composite thermogram shows two exothermic peaks at around 305 °C and 486°C with an enthalpy value of -897.76 J/g for the first peak. These two peaks correspond to the curing of the resin matrix and its degradation. The exothermic peak in DSC at 486°C for SSF/MRR composite is in line with the TGA weight loss of 7% for this composite. On the basis of these data, if one seeks for the production of silica-fiber-reinforced modified phenolic resin preregs, the temperature profile of prepreg heat treatment could be limited to 100°C, a temperature allowing ethanol evaporation and slow initiation of resin curing still remaining at B-stage of curing and which could be consecutively completed under controlled condition at higher temperature. As temperature rises, the modified

resole resin begins to degrade producing a porous carbonaceous char residue which is in good agreement with elsewhere studies [41].

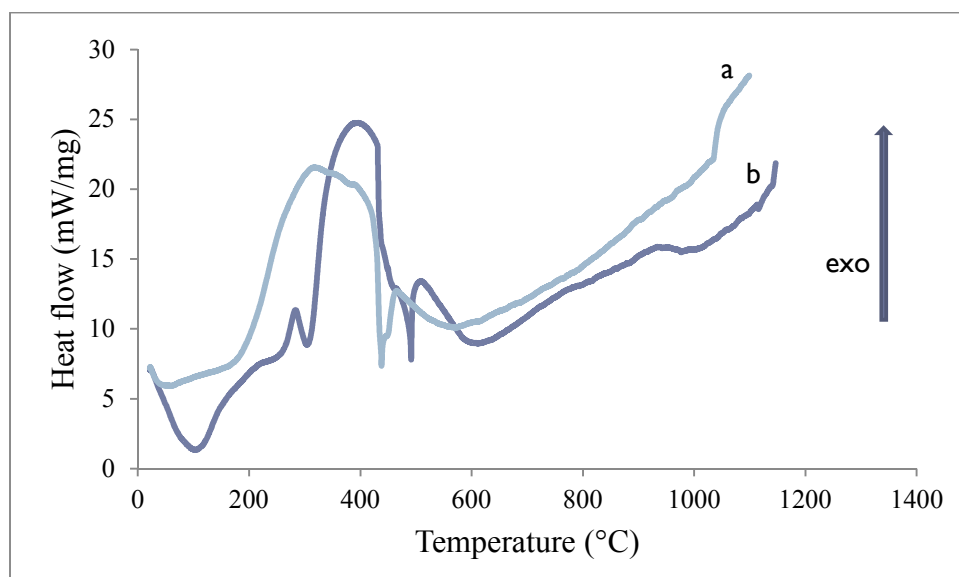


**Figure 13.** DSC thermograms:(a) SSF/MRR composites and (b) modified resole resin.

#### 7-7- Density, porosity and water absorption of SSF/MRR composites.

It is apparently seen that the density of composites increases with the increase in fibre content. The density of composite was 1.21 g/cm<sup>3</sup> at 20% fibre weight ratio, whereas it reached the value of 1.64 g/cm<sup>3</sup> at fibre weight of 65 wt%. This increase was solely arisen from the increasing fibre content in the composites because silica fibre has higher density (2.2 g/cm<sup>3</sup>) than that of the matrix (1.12 g/cm<sup>3</sup>). Density results show that SSF/MRR composite density complies approximately with the rule of mixture. Porosity values seem to be reasonable (except for 40 wt% silica fibre). This can be attributed to relative low melt viscosity of resole resin at pressing temperature which facilitate fibre impregnation and voids reduction (Table 4).

**Table 4.** Gives measured and theoretical density, porosity and water absorption of SSF/MRR composites.

Silica fibre (wt%)	Measured density (g/cm <sup>3</sup> )	Theoretical density (g/cm <sup>3</sup> )	Porosity (% volume)	Water absorption at saturation (wt%)
20	1.21	1.24	2.58	5.68
40	1.29	1.39	5.11	6.01
55	1.51	1.53	1.69	4.88
65	1.64	1.65	0.30	4.31

#### 7-8- Composite water absorption.

From the water absorption curves, it is clear that the absorbed water content increased with an increasing immersion time and the moisture uptake reaches equilibrium moisture content (saturation condition) after fifteen days of immersion for all weight percent of silica fiber content. Figure 14 shows that composites with 40 wt% of silica fibre exhibits the highest water absorption (6.01%) among other composites. Curing of phenolic resin leaves microvoids that contribute to the sites for water absorption in composite material. Moisture absorption into composite materials occurs by three different mechanisms [43-44]. The porosity of the composite, the diffusion of water molecules between polymer chains and the capillary transport at the interfaces between fibres and polymer because of incomplete wetting and impregnation. Water absorption of the SSF/MRR composites seems not only related to their porosity because even with the lowest porosity of 65 wt% SSF/MRR composites, water absorption reached 4.33% this could be attributed to the increase of fiber interface and water absorption of the hydrophilic groups on silica fibre surface and the inability of the low resin content to isolate fibers surface against water penetration and adsorption (Table 4).

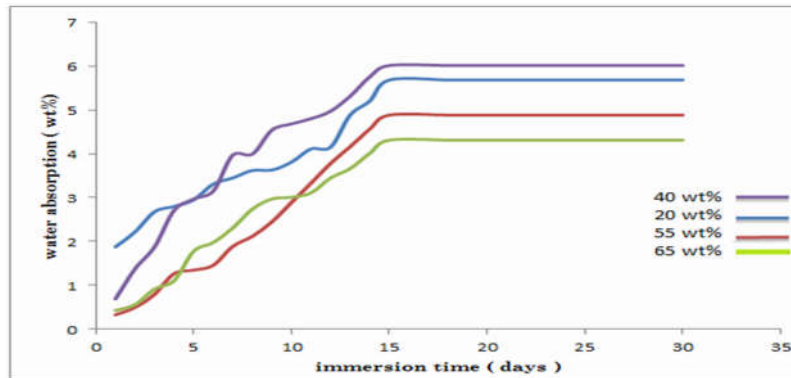


**Figure 14.** Water absorption of SSF/MRR composites versus time and fibre content.

### 7-9- Morphology of the composite.

#### 7-9-1- Optical microscopic examination.

Microscopic images of the sections were apparently clear enough to differentiate short silica fibers from MRR matrix and one can easily distinguish fibers in different orientations and distributed randomly in the matrix as depicted in Figure 15 (a, b, c, d). In addition, one could notice that the fibers and MRR matrix were aggregate as clusters and resin rich regions remained between the fiber bundles (Figure 15: a, b). Some grooves were observed on the surface and that could be attributed to breaking or taking fiber off during polishing operations.

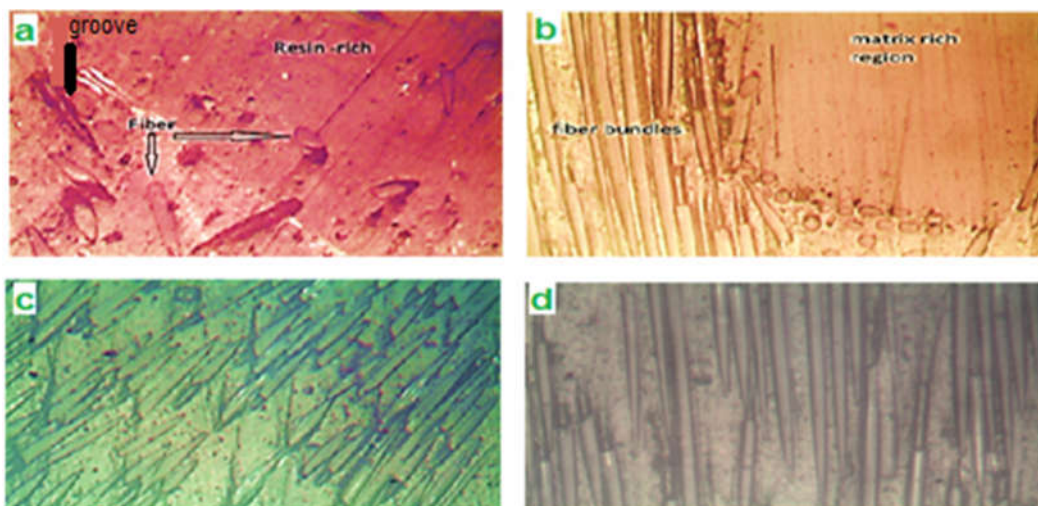


**Figure 15.** (a, b, c, d) Optical micrograph of SSF/MRR composites.

#### 7-9-2- Scanning electron microscopy.

The scanning electron microscopy (SEM) images of the fracture sections of SSF/MRR composites are shown in Figures 16 from (a-i).

The morphology of the composites with 65 wt% (a, b), 55 wt% (c, d), 40 wt% (e, f) and 20 wt% (g, h) SSF content were imaged using scanning electron microscope (SEM) to investigate fibre- matrix bonding because SSF/MRR composite properties are not only related to the cure conditions of matrix and fibre size, but also to the fibre-matrix adhesion, fiber dispersion in the composites and fibre- matrix interfacial interaction [45].

In Figure 16 from (a) to (i), it could be noticed that short silica fibers are randomly dispersed in the resin matrix for almost all fiber content, it could also be seen that SSF fibers are broken or pulled-out as few circle like cavities are formed during sample fracture as depicted in Figure 16 (a, b, e, f). Based on SEM micrographs, one could find some bonded matrix resins on the surfaces of SSF fibers as shown in Figure 16 (a, b, f) for composites including 65 wt% and 55 wt% of SSF fibers respectively. Therefore, SSF fibres wetting by modified resole resin appears poor in certain regions. On the other hand, SEM images of SSF/MRR composites containing respectively 20 wt% and 40 wt% of SSF fibers showed improved and good quality matrix-fiber interface and some resin rich regions as depicted in Figure 16 (e, g, h). This could be related to higher resin content. Figure 16 (c, d) for composites containing 55 wt% of SSF fibers shows obviously an acceptable uniform

distribution of fibers in the matrix, manifested by improved mechanical properties, with a tendency of fiber orientation due to hot pressing. By contrast, composites containing 65 wt% of SSF (Figure 16- a-b) exhibit lack of matrix on fiber surfaces in addition to a non-uniform distribution of fiber and fiber smashing into shorter ones under hot pressing in the mold. These short fibers, under the critical fiber length, randomly dispersed in the resin matrix do not contribute to SSF/MRR composites reinforcement. When composites are under stress, cracks originate from the matrix due to stress concentration caused by defects such as pores and when reaching fiber-matrix interface the fracture will still be in progress [46]. So, the fibers will be pulled out from the matrix because of weak fiber-matrix bonding leaving cavities behind them.

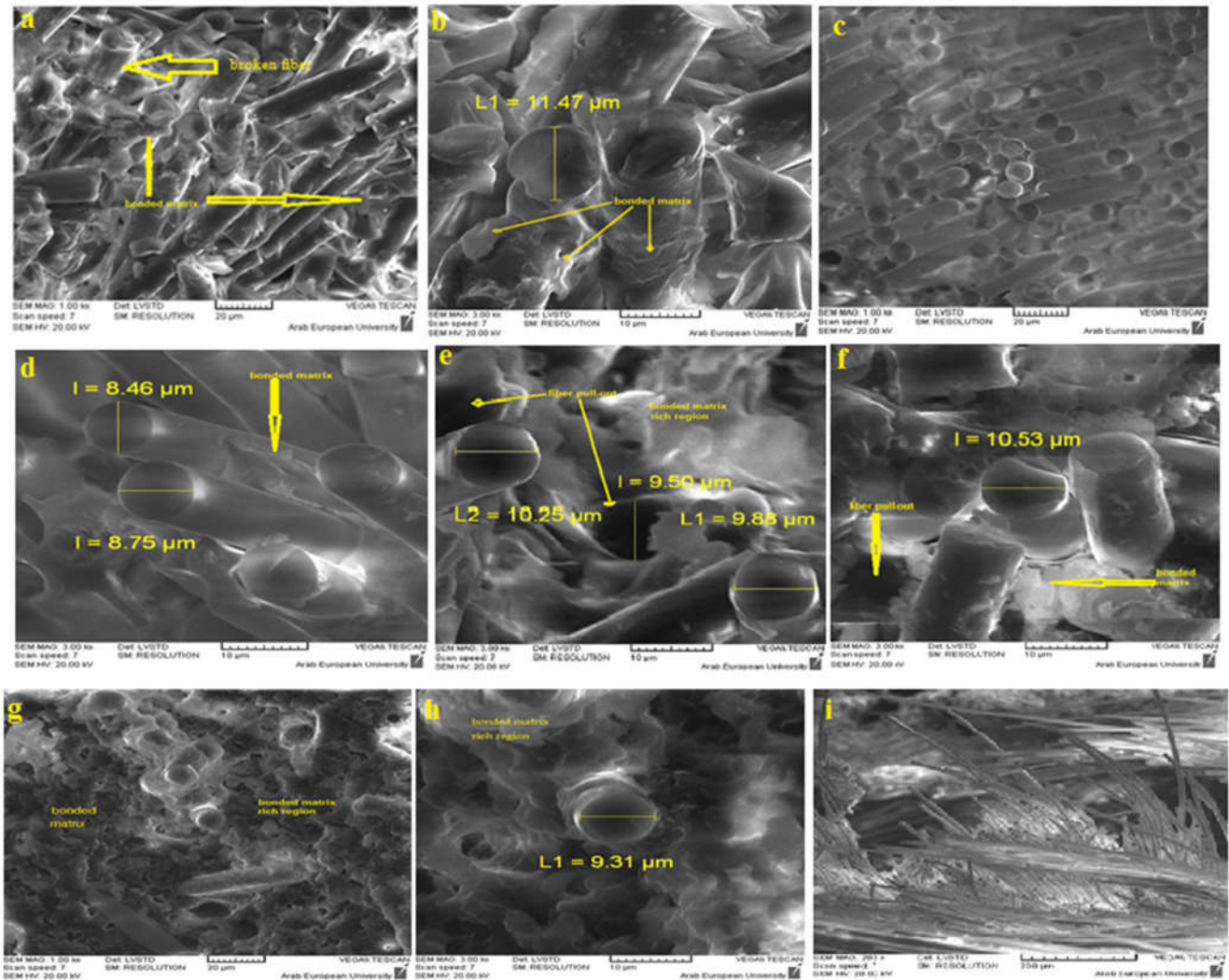


**Figure 16.** SEM images of the fracture surface of SSF/MRR composites prepared with 65 wt% (a, b, i), 55 wt% (c, d), 40 wt% (e, f) and 20 wt% (g, h) short silica fiber respectively.

## Conclusion

The present work focused on the investigation of the influence of short silica fibre content on mechanical and physical properties of short silica fibres modified ammonium resole resin composites. On the basis of the experimental results, the following conclusions can be drawn up:

- The modified resole resin used as a matrix can be loaded with a large range of short silica fibres up to 65 wt% this range may be extended to larger content.
- SSF/MRR composites were prepared through simple and low-cost hot-compression molding without using interfacial promoting bonding agent.
- A good compatibility between PVB and resole resin (mixture of 85 % resole resin and 15 % PVB) was confirmed by FTIR and DSC characterization.
- The density of modified resole resin short silica fibres composites increased with increasing fibre content according to mixture rule.
- The porosity and water absorption of the prepared modified resole resin short silica fibres composites using compression molding were relatively low.
- The characterization of the composites discloses that fiber content exerts a significant effect on the mechanical and physical properties of SSF/MRR composites. The optimum value of mechanical properties was found at 55 wt% of short silica fiber loading.
- The mechanical properties such as tensile strength (28.4MPa), flexural strength (155.03MPa), flexural Young's modulus (12.81GPa), and impact strength (42.04KJ/m<sup>2</sup>) of SSF/MRR composites showed optimum value at 55wt% fibre content.
- The results of thermogravimetric (TGA) analysis showed high residue value of residue (74%) in SSF/MRR composites. This confirms again that SSF/MRR composite is thermally stable and heat resistant composite.
- The microscopic study of modified resole resin short silica fibres composites showed that morphological defects may be responsible for certain low mechanical properties.
- SEM micrographs confirm that the main reasons of failure modes in short silica fibre modified resole resin composites are fibre pull-out, fibre breakage, poor interfacial bonding and debonding.

**Acknowledgments**—The authors are grateful to the Higher Institute for Applied Sciences and Technology (HIASST), Department of Applied Physics, Damascus, Syria for their efficient financial support and facilities.

## References.

1. De S. K., White J. R. Short fibre-polymer composites, Wood head Publishing Limited, (1996).
2. Biolzi L., Castellani L., Pitacco I. Journal of Materials Science. 29(9) (1994) 2507.
3. Shao-Yun Fu., Lauke B. Composites Part A: Applied Science and Manufacturing. 29(5-6) ( 1998 ) 575.
4. Fua S. Y., Lauke B., Maderb E., Yuea C. Y., Hua X. Composites Part A: Applied Science and Manufacturing. 31(10) ( 2000 ) 1125.
5. Heckadka S. S., Nayak S. Y., Narang K., Pant K. V. Journal of Materials 2015 Article ID 957043, (2015)1.
6. Amuthakkannan P., Manikandan V., Winowlin Jappes J.T., Uthayakumar M. Materials Physics and Mechanics. 16 (2013)107.
7. Lee K.S., Lee S.W., Youn J.R., Kang T.J., Chung K. Fibres and Polymers. 2(1) (2001) 41.
8. Bijsterbosch H., Gaymans R. J. Polymer Composites. 16(5) (1995) 363.
9. Ramsteiner F., Theysohn R. Composites Science and Technology. 24(3) (1985) 231.
10. Sarasua J.R., Remiro P.M., Pouyet J. Journal of Materials Science. 30(13) (1995) 3051.
11. Shafizadeh J. E., Guionnet S., Tillman M. S., Seferis J. C. Journal of Applied Polymer Science. 73(4) (1999)505.
12. Winya N., Boonpan A., Prapunkarn K. International Journal of Chemical Engineering and Applications. 4(4) (2013) 234.
13. Cardona F., Kin-Tak A. L., Fedrigo J. Journal of Applied Polymer Science. 123(4) (2012) 2131.
14. Deanin R.D., Crugnola A.M., Gould, R.F. Toughness and brittleness of plastics. ACS publications, Advances in chemistry Vol.154, (1976).
15. Kaynak C., Cagatay O. Polymer Testing. 25(3) (2006) 296.
16. Verma A.P., Vishwanath B., Kameswara Rao C.V.S. Wear. 193(2) (1996) 193.

17. Ismail I.N., Ishak Z.A.M., Jaafar M.F., Omar S., ZainalAbidin M.F., Ahmad Marzuki H.F. *Solid State Science and Technology*. 17(1) (2009) 155.
18. Kang T.J., Hwang S. D. *Polymers and polymer composites*. 4(4) (1996) 217.
19. Bin L., Chang-Rui Z., Si-Qing W., Feng C., Yong-Gang J. *Refractories and Industrial Ceramics*. 48(4) (2007) 280.
20. Thomas S., Joseph K., Malhorta S. K., Koichi G., Sreekala M. S. *Polymer Composites. Volume1, Macro- and Microcomposites*, Wiley-VCH, (2012).
21. Rauch H. W., Sutton Sr. W. H., McCreight L. R. *Ceramic fibres and fibrous composite materials (Refractory Materials 3)*. Published by Academic Press, (1968).
22. George L. *Handbook of composites*, Springer, (1982).
23. Thomas S., Sreekala M.S., Jayamol G., Kumaranc M.G. *Composites Science and Technology*. 62(3) (2002) 339.
24. Hine P. J., Davidson N. D., Ward I. M. *Composite science and technology*. 53(2) (1995) 125.
25. Fu S.Y., Hu X.Y., Chee Y. *Composite science and technology*. 59(10) (1999) 1533.
26. Venkata R. G., Mithil K. N., Venkata N. S. *Journal of Reinforced Plastics and Composites*. 28(21) ( 2009) 2605.
27. Botev M., Betchev H., Bikiaris D., Panayiotou C. *Journal of Applied Polymer Science*. 74(3) (1999) 523.
28. Agarwal B. D., Broutman L. J. *Analysis and performance of fibre composites*, New York, John Wiley and Sons, (1990).
29. Polyvinylbutyral. MowitalPioloform Brochure 2013, [www.kuraray.eu](http://www.kuraray.eu).
30. High fiberglass silica cloth .[www.sdcjxcl.com](http://www.sdcjxcl.com).
31. Standard Test Method for Moisture Absorption Properties and Equilibrium Conditioning of Polymer Matrix Composite Materials. ASTM D 5229/D 5229M, (2004).
32. Standard Test Methods for Void Content of Reinforced Plastics. D 2734, (2003).
33. Jun-ichi O., Wataru O., Asao O. *Carbon*. 38(10) (2000) 1515.
34. Zhiqin C., Yangfei C., Hongbo L. *Advanced Materials Research*. 631-632 (2013) 104.
35. Ansari S. I., Ali P., Srivastava S., Ahmad Khan I. *Oriental journal of chemistry*. 32(1) (2016) 429.
36. Nirmal C., Maithi S.N., Padmavathi T. *High Performance Polymers*. 18(2006) 57.
37. Kumar K. S. S., Nair C. P. R., Ninan K. N. *Polymer advanced Technologies*. 19(7) (2008) 895.
38. Thomas S., Seena J., Sreekala M.S., Oommen Z., Koshy P. *Composites Science and Technology*. 62(14) (2002) 1857.
39. Agarwal G., Patnaik A., Sharma R. K. *Journal of Engineering Science and Technology*. 9(5) (2014) 590.
40. Sebrekoska V., Dimeski D., Bogoeva G. G. *Journal of the Serbian Chemical Society*. 74(4) (2009) 441.
41. Lee D. G., Choe J., Kim, M. *Composite Structures*. 148(2016) 191.
42. Kimberly A. T., Tony E. S. *Carbon*. 33(11) (1995) 1509.
43. Parameswaran P. S., Bhuvaneshwary M. G., Eby T. *TJournal of Applied Polymer Science*. 113(2) (2009) 802.
44. Andreopoulos A. G., Tarantili P. A. *Journal of Applied Polymer Science*. 70(4) (1998) 747.
45. Drzal L. T. *Vacuum*. 41(7-9) (1990) 1615.
46. Sha J.J., Dai J.Y., Wei Z.Q., Li J., Hausherr J-M., Krenkel, W. *Journal of Composite Materials*. 0(0) (2013)1.

(2017) ; <http://www.jmaterenvirosci.com>